Applied Physics Letters

Optics of epitaxial strained strontium titanate films

Cite as: Appl. Phys. Lett. **117**, 082901 (2020); https://doi.org/10.1063/5.0021461
Submitted: 11 July 2020 . Accepted: 13 August 2020 . Published Online: 24 August 2020

M. Tyunina, N. Nepomniashchaia, V. Vetokhina, and A. Dejneka

Applied Physics Letters ARTICLE scitation.org/journal/apl

Optics of epitaxial strained strontium titanate films

Cite as: Appl. Phys. Lett. **117**, 082901 (2020); doi: 10.1063/5.0021461
Submitted: 11 July 2020 · Accepted: 13 August 2020 ·
Published Online: 24 August 2020

M. Tyunina,[1,2,a)] N. Nepomniashchaia,[2] V. Vetokhina,[2] and A. Dejneka[2]

AFFILIATIONS

[1]Microelectronics Research Unit, Faculty of Information Technology and Electrical Engineering, University of Oulu, P. O. Box 4500, FI-90014 Oulu, Finland
[2]Institute of Physics of the Czech Academy of Sciences, Na Slovance 2, 18221 Prague, Czech Republic

[a)]**Author to whom correspondence should be addressed:** marina.tjunina@oulu.fi

ABSTRACT

Diverse effects of lattice strain on the optical properties in the near-infrared to vacuum ultraviolet spectral range are experimentally revealed in cube-on-cube-type epitaxial perovskite $SrTiO_3$ films grown on compressive substrate. Compared to the reference crystal, the tetragonal antiferrodistortive film exhibits spectral blueshifts, which are consistent with the theoretically predicted bandgap widening. In addition to this strain-induced interband effect, the peculiar near-edge absorption and smearing of interband transitions are found. It is shown that Fröhlich-type electron–phonon coupling can be enhanced by strain and lead to this behavior. It is suggested that electron–phonon interactions can play an important role in optical properties of ferroelectric films and deserve further studies.

Strontium titanate ($SrTiO_3$, STO) is a representative of perovskite oxide ferroelectrics (FEs). These materials are wide bandgap insulators and transparent in the spectral range from the mid-infrared to the ultraviolet, where their index of refraction can be tuned by electric field, stress, or light. These optical properties enable diverse optoelectronic and photonic devices, most advanced of which employ single-crystal-type epitaxial films.[1–5] In such films, film-substrate mismatches in crystal symmetries, lattice parameters, and thermal expansion coefficients can lead to lattice stains and strain-induced phases, which have no analogs in prototype crystals.[6–9] First-principles modeling suggests that epitaxial strain can also affect bandgap energy, elasto-optic coefficients, and electrooptic coefficients.[10–16] However, the experimentally observed optical properties of epitaxial films do not always agree with modeling and are scattered and often poorly understood.[2–5,17,18] Apart from unintentional technological issues, this disparity indicates insufficient knowledge of optical phenomena in epitaxial films and creates a bottleneck for potential applications. Here, we aim to better clarify these phenomena in epitaxial strained films of representative STO.

Because epitaxial STO films can be grown on commercial silicon substrates, they are of great practical importance for integrated photonics and electronics.[19] Substrate-induced biaxial in-plane misfit strain is compressive in thin STO films on Si, where the substrate-ensured in-plane lattice parameter is ∼3.840 Å. In this work, we use $(001)(La_{0.3}Sr_{0.7})(Al_{0.65}Ta_{0.35})O_3$ (LSAT) substrates to enable the in-plane lattice parameter of 3.868 Å and cube-on-cube epitaxial growth of in-plane compressed STO films, resembling those on Si.

Our experimental studies reveal that in addition to theoretically predicted strain-induced changes of band structure, also less recognized strain-enhanced electron–phonon coupling can play an essential role in optical behavior of epitaxial STO films.

The theoretical STO/LSAT misfit strain is $s_a = (a_{LSAT}/a_{STO} - 1) \approx -0.95\%$ where $a_{LSAT} = 3.868$ Å and $a_{STO} = 3.905$ Å are the lattice parameters of LSAT and STO, respectively. For the coherent strained (001) STO film on (001) LSAT, the in-plane lattice parameters are similar and equal to $a = a_{LSAT}$ and the out-of-plane lattice parameter c is elongated: $c = a_{STO}\cdot[1 - (2c_{12}/c_{11})\cdot s_a] \approx 3.927$ Å, where $c_{11} = 3.48 \times 10^{11}$ N/m^2 and $c_{12} = 1.03 \times 10^{11}$ N/m^2 are the elastic constants of STO.[20] As found recently,[9] such tetragonal fully strained STO/LSAT films can grow to thickness of ∼100 nm, above which the misfit relaxation occurs.

STO films with a thickness of ∼80 nm were grown by pulsed lased deposition using an excimer KrF laser (Compex 205 F, wavelength 248 nm, energy density 2 J/cm^2, pulse repetition rate 5 Hz) on as-received 10×10 mm^2 single-crystal epitaxially polished (001) LSAT substrates (MTI Corp.). A dense ceramic pellet of STO (synthesized in the Institute of Solid State Physics, University of Latvia) was used as a target. A substrate temperature, monitored by a pyrometer, was 973 K during deposition and lowered at a rate of 5 K min^{-1} during post-deposition cooling. Pressure of oxygen ambience was 20 Pa and 800 Pa during deposition and cooling, respectively. High-resolution

x-ray diffraction (HRXRD) and reflectometry studies were performed on a D8 Discover diffractometer (Bruker corporation) using Cu Kα radiation. The diffraction and reflectometry data were fitted using LEPTOS software.

XRD analysis evidenced a cube-on-cube-type epitaxy (supplementary material Fig. S1). The STO films are coherent to STO and tetragonal. The lattice parameters are nearly equal to the theoretically estimated ones, although indications of partial relaxation of misfit strain can be seen [supplementary material Fig. S1(c)]. According to the state-of-the-art strain-temperature phase diagram,[9] our tetragonal films are expected to adopt a room-temperature non-polar antiferrodistortive (AFD) phase. Unstressed bulk STO is cubic paraelectric at room temperature and undergoes the low-temperature paraelectric-to-AFD phase transition, which can produce changes in the electronic band structure and, consequently, optical properties.[10,21,22] However, as found experimentally, these changes are negligible in bulk.[23,24] We note that the properties of the misfit-induced AFD phase in epitaxial films differ from those in bulk AFD STO because of anisotropic lattice strain, which is imposed by the substrate in epitaxial films.[10]

The STO/LSAT films experience in-plane compressive and out-of-plane tensile strains. To elucidate optical effects of epitaxial strain, we investigated the optical absorption coefficient α and dielectric function ($\varepsilon^* = \varepsilon_1 + i\varepsilon_2$) in the tetragonal AFD film and a reference epitaxially polished (001) STO crystal (MTI Corp.). The optical constants and dielectric functions were determined by variable angle spectroscopic ellipsometry on a J. A. Woollam VUV ellipsometer at room temperature and photon energies $E = 0.7$–8.8 eV. The ellipsometric spectra were acquired in an atmosphere of dry nitrogen at five angles of incidence (55°–80° with 5° step) with an energy step of 0.02 eV using averaging over 200–400 optical cycles. The optical constants of the film, crystal, and LSAT substrate were extracted from the spectra of ellipsometric angles using a commercial WVASE32 software package (supplementary material Fig. S2). More details can be found elsewhere.[17]

Absorption spectra [Fig. 1(a)] show that the AFD film is highly transparent at the energies $E < 3.5$ eV, in contrast to substantial absorption for this spectral range in non-stoichiometric STO films.[18,25] The film's spectrum is clearly shifted to higher photon energies compared to that of the crystal, and the blueshift is accompanied by a relative suppression or smearing of the spectral features. This behavior indicates an uplift of the conduction band and changes of the interband transitions in the film.

First, we analyzed the absorption edge using the commonly applied Tauc-type plots for direct (1) and indirect (2) gaps, and the Urbach rule for the absorption tail (3)[26–29]

$$(\alpha E)^2 \propto (E - E_d), \tag{1}$$

$$(\alpha E)^{1/2} \propto (E - E_i), \tag{2}$$

$$\alpha = \alpha_0 \exp\left[\frac{\sigma(E - E_0)}{k_B T}\right]. \tag{3}$$

Here, E_d and E_i are the gap energies, k_B is the Boltzmann constant, and the parameters α_0, σ, and E_0 describe the absorption tail. A good indirect-gap fit with $E_i \approx 3.22$ eV is obtained for the crystal [Fig. 1(b)], in agreement with the well-established behavior.[23,24,30,31] Although indirect-gap fitting with $E_i \approx 3.45$ eV can be performed for the film as well [Fig. 1(b)], the fit is rather inaccurate because of a steep Urbach tail therein [Fig. 1(c)]. The tail parameter $\sigma \approx 0.3$ in the film is significantly enhanced compared to $\sigma \approx 0.06$ in bulk.[31] This observation may indicate an enhancement of the electron–phonon interactions in the film.[32] Good direct-gap fits are obtained for $E > 4$ eV, far from the edge [Figs. 1(d) and 1(e)]. It is therefore likely that the bandgap is indirect in the AFD film, similarly to the low-temperature AFD and high-temperature paraelectric phases of bulk STO. The fitted energies $E_d \approx 3.85$ eV in the crystal and $E_d \approx 3.97$ eV in the film suggest at least ~0.1 eV blueshift, which is consistent with the theoretically predicted widening of the optical gaps in misfit-strained epitaxial AFD phase.[10]

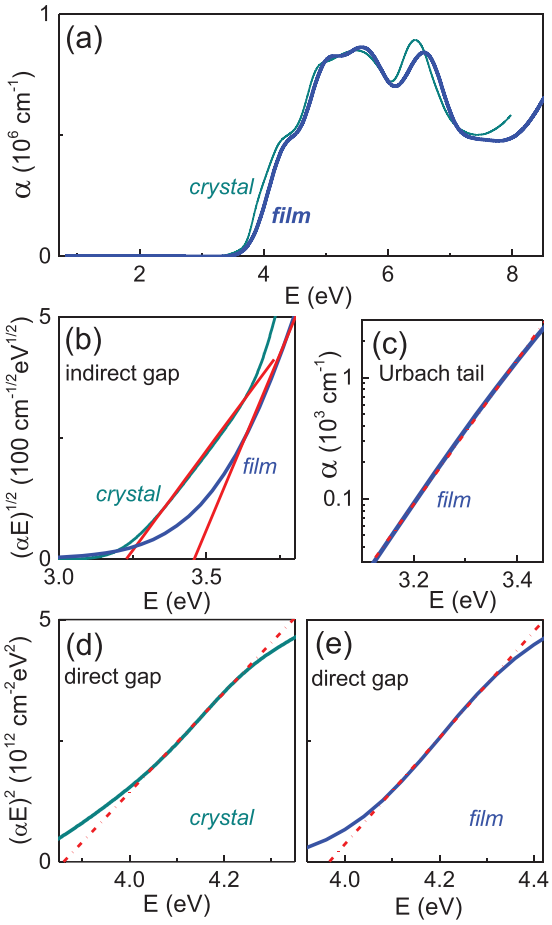

FIG. 1. (a) Absorption coefficient α as a function of photon energy in the film (thick curve) and reference crystal (thin curve). (b) Tauc plots for indirect bandgap. Solid lines show fits. (c) Urbach tail in the film. Note logarithmic scale for α. The dashed line shows fit. (d) and (e) Plots for direct gaps. Dashed lines show fits.

Next, we examined critical points (CPs) to unveil the changes of the interband transitions in more detail.[33–36] For a two-dimensional CP, the second derivative of the dielectric function takes the form (4),

$$\frac{d^2\varepsilon}{dE^2} = \frac{A\exp(i\phi)}{(E - E_{CP} + i\Gamma)^2}. \tag{4}$$

Here A, E_{CP}, Γ, and φ are the amplitude, energy, width, and phase angle of the CP line, respectively. For simplicity, the phase angles are

assumed to be $\varphi = 0$, 0.5π, π, and 1.5π. The derivatives $d^2\varepsilon_1/dE^2$ and $d^2\varepsilon_2/dE^2$ were extracted from the dielectric functions (Fig. 2). In the film, the CP lines are mainly similar to those in the crystal but clearly blueshifted, in agreement with the predicted bandgap behavior.[10]

Notably, compared to the main broad asymmetric CP line (~3.8 eV), which was recently reported for bulk STO,[32] our measurements resolved two narrower symmetric CP lines (a strong one at ~3.8 eV and a weaker one at ~4.2 eV) in the crystal [Figs. 3(a) and 3(b)]. Our observations agree well with those in Ref. 36. The strong CP (~3.8 eV) of the crystal shifts (to ~4.0 eV) in the film, in accordance with the theoretical expectation.[10] Unexpectedly, this line significantly weakens and broadens in the film [Figs. 3(a) and 3(b)]. The blueshift and smearing are also well seen for other CPs (see, for instance, CPs ~6.35 eV in the crystal and ~6.50 eV in the film). Because such a smearing was not observed in the low-temperature AFD phase of the crystals, it may be related to the presence of strain in the AFD film.

We suggest that the smearing may result from strain-enhanced electron–phonon coupling. As shown experimentally, the frequencies ω of the lowest polar phonon mode (soft mode) are higher in the compressively strained tetragonal STO films than in bulk STO for all temperatures.[37–40] Whereas the frequency increases (soft mode hardens) with temperature as ($\omega^2 \propto T$) to 130 cm^{-1} at $T = 700$ K in bulk STO,

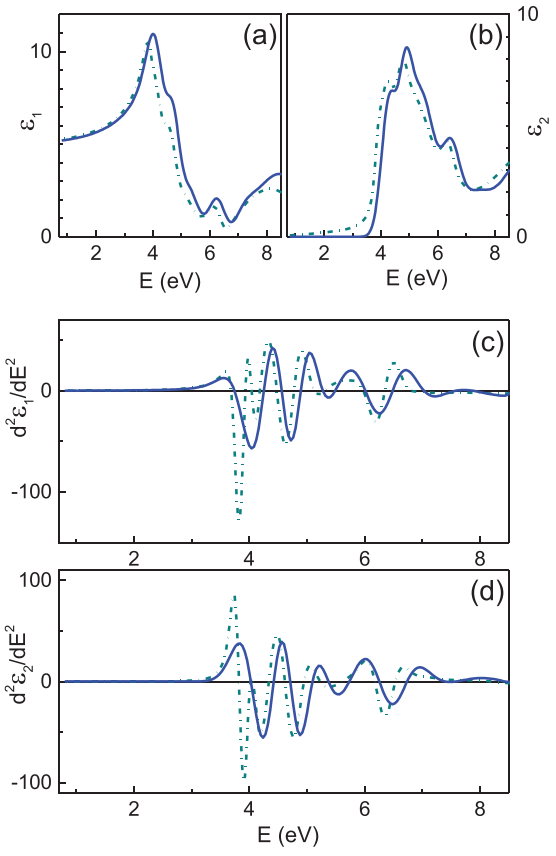

FIG. 2. The (a) real and (b) imaginary parts of the dielectric function and their second derivatives (c) and (d) in the film (solid curves) and crystal (dashed curves).

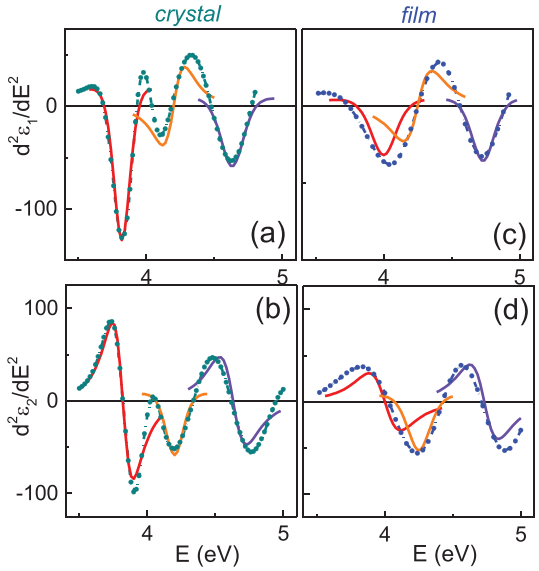

FIG. 3. Second derivatives of the (a) and (c) real and (b) and (d) imaginary parts of the dielectric function in the (a) and (b) crystal and (c) and (d) film. Experimental data are shown by solid circles. Thin curves show CP lines.

frequencies as high as 125–135 cm^{-1} were found at a lower temperature of 300 K in the strained films. We note that strain-induced soft-mode hardening was not captured by theoretical calculations.

Taking into account that Fröhlich-type electron–phonon interactions are generally strong in ionic crystals, such interactions may be substantial in STO as well. The electron–phonon coupling constant F_{ep} is known to increase with frequency: [$F_{ep} \propto (\omega)^{1/2}$].[35] Thus, the strain-induced soft-mode hardening can lead to an enhanced electron–phonon coupling in the AFD films. This enhancement may be responsible for the observed CP smearing, steep Urbach tail, and progressive smearing with increasing temperature (supplementary material Fig. S3) in the film. We note that the Fröhlich electron–phonon interaction can also cause the spectral blueshifts, but their magnitude is very small, only 0.01–0.02 eV for the phonon hardening from 100 to 120 cm^{-1}. The phonon-frequency enlargement from 100 cm^{-1} in bulk to 125 cm^{-1} in the film therefore cannot explain the large observed blueshifts. Distinct interband effects are obviously present in the film.

The suggested strain-enhanced electron–phonon coupling may have implications for optical properties of not only epitaxial, but also polycrystalline STO films, where the substrate and crystal grains (grain boundaries) are sources of lattice strains. In particular, the discussed CP smearing is consistent with the experimental observations in such films.[36] Because electron–phonon coupling can be strong in all perovskite oxide ferroelectrics, strain-induced enhancement of this coupling may play an important role in optical behavior of ferroelectric films. We also emphasize that electron–phonon interactions may significantly contribute to elasto- and electro-optic coefficients above their interband levels,[41,42] which is of high interest for applications. Therefore, electron–phonon coupling in ferroelectric films requires more detailed experimental investigations and comprehensive theoretical modeling.

In conclusion, the optical absorption and dielectric functions were experimentally investigated in the spectral range of 0.7–8.8 eV in epitaxially strained tetragonal AFD STO film. Compared to the reference unstressed crystal, the spectral blue-shifts of ∼0.2 eV are detected in the film and ascribed to the theoretically predicted strain-induced bandgap widening. Additionally, the peculiar near-edge absorption tail and smearing of interband transitions are observed and suggested to originate from strain-enhanced electron–phonon coupling. It is proposed that electron–phonon coupling can have significant effects on optical behavior of ferroelectric films and deserves further investigations.

See the supplementary material for XRD scans and details of ellipsometric analyses.

The authors would like to thank T. Kocourek, O. Pacherova, and D. Chvostova for their contributions and advise. The authors acknowledge support from the Czech Science Foundation (Grant No. 19-09671S) and the European Structural and Investment Funds and the Ministry of Education, Youth and Sports of the Czech Republic through Programme "Research, Development and Education" (Project No. SOLID21-CZ.02.1.01/0.0/0.0/16_019/0000760).

DATA AVAILABILITY

The data that support the findings of this study are available from the corresponding author upon reasonable request.

REFERENCES

[1]B. W. Wessels, "Ferroelectric epitaxial thin films for integrated optics," Annu. Rev. Mater. Res. **37**, 659 (2007).
[2]S. Abel, T. Stöferle, C. Marchiori, D. Caimi, L. Czornomaz, M. Stuckelberger, M. Sousa, B. J. Offrein, and J. Fompeyrine, "A hybrid barium titanate–silicon photonics platform for ultraefficient electro-optic tuning," J. Lightwave Technol. **34**, 1688 (2016).
[3]D. Sando, Y. Yang, C. Paillard, B. Dkhil, L. Bellaiche, and V. Nagarajan, "Epitaxial ferroelectric oxide thin films for optical applications," Appl. Phys. Rev. **5**, 041108 (2018).
[4]S. Abel, T. Stöferle, C. Marchiori, C. Rossel, M. D. Rossell, R. Erni, D. Caimi, M. Sousa, A. Chelnokov, B. J. Offrein, and J. Fompeyrine, "A strong electro-optically active lead-free ferroelectric integrated on silicon," Nat. Commun. **4**, 1671 (2013).
[5]S. Abel, F. Eltes, J. E. Ortmann, A. Messner, P. Castera, T. Wagner, D. Urbonas, A. Rosa, A. M. Gutierrez, D. Tulli, P. Ma, B. Baeuerle, A. Josten, W. Heni, D. Caimi, L. Czornomaz, A. A. Demkov, J. Leuthold, P. Sanchis, and J. Fompeyrine, "Large Pockels effect in micro- and nanostructured barium titanate integrated on silicon," Nat. Mater. **18**, 42 (2019).
[6]N. A. Pertsev, A. G. Zembilgotov, and A. K. Tagantsev, "Effect of mechanical boundary conditions on phase diagrams of epitaxial ferroelectric thin films," Phys. Rev. Lett. **80**, 1988 (1998).
[7]N. A. Pertsev, A. K. Tagantsev, and N. Setter, "Phase transitions and strain-induced ferroelectricity in $SrTiO_3$ epitaxial thin films," Phys. Rev. B **61**, R825 (2000).
[8]J. Li, Z. Shan, and E. Ma, "Elastic strain engineering for unprecedented materials properties," MRS Bull. **39**, 108 (2014).
[9]T. Yamada, B. Wylie-van Eerd, O. Sakata, A. K. Tagantsev, H. Morioka, Y. Ehara, S. Yasui, H. Funakubo, T. Nagasaki, and H. J. Trodahl, "Phase transitions associated with competing order parameters in compressively strained $SrTiO_3$ thin films," Phys. Rev. B **91**, 214101 (2015).
[10]R. F. Berger, C. J. Fennie, and J. B. Neaton, "Band gap and edge engineering via ferroic distortion and anisotropic strain: The case of $SrTiO_3$," Phys. Rev. Lett. **107**, 146804 (2011).
[11]F. Wang, I. Grinberg, and A. M. Rappe, "Band gap engineering strategy via polarization rotation in perovskite ferroelectrics," Appl. Phys. Lett. **104**, 152903 (2014).
[12]L. Chen, Y. Yang, Z. Gui, D. Sando, M. Bibes, X. K. Meng, and L. Bellaiche, "Large elasto-optic effect in epitaxial $PbTiO_3$ films," Phys. Rev. Lett. **115**, 267602 (2015).
[13]D. Sando, Y. Yang, E. Bousquet, C. Carretero, V. Garcia, S. Fusil, D. Dolfi, A. Barthelemy, Ph. Ghosez, L. Bellaiche, and M. Bibes, "Large elasto-optic effect and reversible electro-chromism in multiferroic $BiFeO_3$," Nat. Commun. **7**, 10718 (2016).
[14]K. D. Fredrickson, V. V. Vogler-Neuling, K. J. Kormondy, D. Caimi, F. Eltes, M. Sousa, J. Fompeyrine, S. Abel, and A. A. Demkov, "Strain enhancement of the electro-optical response in $BaTiO_3$ films integrated on Si(001)," Phys. Rev. B **98**, 075136 (2018).
[15]A. K. Hamze and A. A. Demkov, "First-principles study of the linear electro-optical response in strained $SrTiO_3$," Phys. Rev. Mater. **2**, 115202 (2018).
[16]C. Paillard, S. Prokhorenko, and L. Bellaiche, "Strain engineering of electro-optic constants in ferroelectric materials," npj Comput. Mater. **5**, 6 (2019).
[17]A. Dejneka, D. Chvostova, O. Pacherova, T. Kocourek, M. Jelinek, and M. Tyunina, "Optical effects induced by epitaxial tension in lead titanate," Appl. Phys. Lett. **112**, 031111 (2018).
[18]R. J. Cottier, N. A. Steinle, D. A. Currie, and N. Theodoropoulou, "Band gap tuning of epitaxial $SrTiO_{3-\delta}$/Si(001) thin films through strain engineering," Appl. Phys. Lett. **107**, 221601 (2015).
[19]R. A. McKee, F. J. Walker, and M. F. Chisholm, "Crystalline oxides on silicon: The first five monolayers," Phys. Rev. Lett. **81**, 3014 (1998).
[20]*Landolt-Börnstein, Numerical Data and Functional Relationships in Science and Technology, New Series, Group III, Crystal and Solid State Physics*, edited by K. H. Hellwege and A. M. Hellwege (Springer, Berlin, 1981).
[21]E. Heifets, E. Kotomin, and V. A. Trepakov, "Calculations for antiferrodistortive phase of $SrTiO_3$ perovskite: Hybrid density functional study," J. Phys. **18**, 4845–4851 (2006).
[22]P. Galinetto, F. Rossella, G. Samoggia, V. Trepakov, E. Kotomin, E. Heifets, P. Markovin, and L. Jastrabik, "Structural phase transition and photo-charge carrier transport in $SrTiO_3$," Ferroelectrics **337**, 179 (2006).
[23]V. Trepakov, A. Dejneka, P. Markovin, A. Lynnyk, and L. Jastrabik, "A "soft electronic band" and the negative thermooptic effect in strontium titanate," New J. Phys. **11**, 083024 (2009).
[24]A. Dejneka, V. Trepakov, and L. Jastrabik, "Spectroscopic ellipsometry of $SrTiO_3$ crystals applied to antiferrodistortive surface phase transition," Phys. Status Solidi B **247**, 1951 (2010).
[25]Y. S. Kim, J. Kim, S. J. Moon, W. S. Choi, Y. J. Chang, J.-G. Yoon, J. Yu, J.-S. Chung, and T. W. Noh, "Localized electronic states induced by defects and possible origin of ferroelectricity in strontium titanate thin films," Appl. Phys. Lett. **94**, 202906 (2009).
[26]J. Tauc, R. Grigorovici, and A. Vancu, "Optical properties and electronic structure of amorphous germanium," Phys. Status Solidi B **15**, 627 (1966).
[27]J. Tauc, "Optical properties and electronic structure of amorphous Ge and Si," Mater. Res. Bull. **3**, 37 (1968).
[28]J. I. Pankove, *Optical Processes in Semiconductors* (Dover, New York, 1975).
[29]N. V. Kurik and U. Rule, Phys. Status Solidi A **8**, 9 (1971).
[30]D. J. Kok, K. Irmscher, M. Naumann, C. Guguschev, Z. Galazka, and R. Uecker, "Temperature-dependent optical absorption of $SrTiO_3$," Phys. Status Solidi A **212**, 1880 (2015).
[31]P. K. Gogoi and D. Schmidt, "Temperature-dependent dielectric function of bulk $SrTiO_3$: Urbach tail, band edges, and excitonic effects," Phys. Rev. B **93**, 075204 (2016).
[32]M. Rossle, C. N. Wang, P. Marsik, M. Yazdi-Rizi, K. W. Kim, A. Dubroka, I. Marozau, C. W. Schneider, J. Humlicek, D. Baeriswyl, and C. Bernhard, "Optical probe of ferroelectric order in bulk and thin-film perovskite titanates," Phys. Rev. B **88**, 104110 (2013).
[33]P. Lautenschlager, M. Garriga, L. Vina, and M. Cardona, "Temperature dependence of the dielectric function and interband critical points in silicon," Phys. Rev. B **36**, 4821 (1987).
[34]P. Lautenschlager, M. Garriga, S. Logothetidis, and M. Cardona, "Interband critical points of GaAs and their temperature dependence," Phys. Rev. B **35**, 9174 (1987).

[35]P. Y. Yu and M. Cardona, *Fundamentals of Semiconductors, Physics and Materials Properties* (Springer, Berlin, 1996).
[36]S. Zollner, A. A. Demkov, R. Liu, P. L. Fejes, and R. B. Gregory, "Optical properties of bulk and thin-film $SrTiO_3$ on Si and Pt," J. Vac. Sci. Technol., B **18**, 2242 (2000).
[37]T. Yamada, J. Petzelt, A. K. Tagantsev, S. Denisov, D. Noujni, P. K. Petrov, A. Mackova, K. Fujito, T. Kiguchi, K. Shinozaki, N. Mizutani, V. O. Sherman, P. Muralt, and N. Setter, "In-plane and out-of-plane ferroelectric instabilities in epitaxial $SrTiO_3$ Films," Phys. Rev. Lett. **96**, 157602 (2006).
[38]D. Nuzhnyy, J. Petzelt, S. Kamba, X. Marti, T. Cechal, C. M. Brooks, and D. G. Schlom, "Infrared phonon spectroscopy of a compressively strained (001) $SrTiO_3$ film grown on a (110) $NdGaO_3$ substrate," J. Phys. **23**, 045901 (2011).
[39]J. Petzelt and S. Kamba, "Far-infrared and terahertz spectroscopy of ferroelectric soft modes in thin films: A review," Ferroelectrics **503**, 19 (2016).
[40]P. Marsik, K. Sen, J. Khmaladze, M. Yazdi-Rizi, B. P. P. Mallett, and C. Bernhard, "Terahertz ellipsometry study of the soft mode behavior in ultrathin $SrTiO_3$ films," Appl. Phys. Lett. **108**, 052901 (2016).
[41]M. DiDomenico, Jr. and S. H. Wemple, "Optical properties of perovskite oxides in their paraelectric and ferroelectric phases," Phys. Rev. **166**, 565 (1968).
[42]S. H. Wemple and M. DiDomenico, "Theory of the elasto-optic effect in nonmetallic crystals," Phys. Rev. B **1**, 193 (1970).